JOURNAL OF CATALYSIS 19, 176–194 (1970)

The Surface Reaction Between Manganese Dioxide and 1,1-Diphenyl-2-picrylhydrazine. Two Type EPR Methods for the Estimation of Active Surface Areas of Oxides

A. T. T. OEI AND J. L. GARNETT

Department of Physical Chemistry, The University of New South Wales, N.S.W. Kensington, 2033, Australia

Received November 26, 1968

The reaction between 1,1-diphenyl-2-picrylhydrazine ($DPPH_2$) in benzene and MnO_2 has been investigated in detail by electron paramagnetic resonance spectroscopy. It is found that a stationary concentration of the hydrazyl (DPPH) is produced and varies asymtotically with volume, mass, and initial $DPPH_2$ concentration. Using this procedure, the active oxygen surface area of the MnO_2 used has been determined (41.5 m^2/g). A confirmatory surface area measurement (46 m^2/g) has also been made using an independent procedure involving DPPH adsorption. The results have been compared with a BET value of 61 m^2/g. DPPH adsorption on the surface is the limiting factor in the $DPPH_2$–MnO_2 reaction since this process results in competitive displacement of $DPPH_2$ from the surface. This effect is significant for concentrations of DPPH above 0.6×10^{-3} moles $liter^{-1}$. The kinetics for the reaction between $DPPH_2$ and MnO_2 follow the equation:

$$\frac{1}{C_0 - C_{De}} \ln \frac{C_0 - C_D}{C_{De} - C_l} = \lambda t + I,$$

where λ and I are constants, C_0 is the initial $DPPH_2$ concentration, C_{De} and C_D are the stationary instantaneous concentrations of DPPH, respectively, and t is time. λ varies linearly with $1/V$ and m, according to the equations $\lambda = 0.34\ (V^{-1}) + 30.6$ and $\lambda = 1332\ m + 35.6$ $moles^{-1}$ liters min^{-1}, where V is the volume in liters, and m, the mass of oxide in grams. Finally, λ obeys the Arrhenius equation giving an apparent activation energy of 5.1 kcal/mole and a frequency factor of 1.84×10^6. $moles^{-1}$ liters min^{-1}. A mechanism for the $DPPH_2$–MnO_2 reaction is proposed involving π-complex adsorbed intermediates. The possible variables affecting the application of the above two methods for general active surface area determination are discussed.

INTRODUCTION

The conversion of 1,1-diphenyl-2-picrylhydrazine ($DPPH_2$) to the corresponding radical (DPPH) is normally effected by PbO_2 (*1*). A particularly active PbO_2 can be prepared from lead tetraacetate by the method of Kuhn and Manner (*2*). The conversion can also be achieved by $PtO_2 \cdot 2H_2O$, $IrO_2 \cdot 2H_2O$, $RuO_2 \cdot H_2O$ and oxygen-poisoned prereduced platinum oxide (*3*). The possibility of using the reaction as a method for estimating the active oxygen content of the metal oxides of platinum, iridium, and ruthenium has been considered (*3*).

In addition to these Group VIII transition metal oxides and PbO_2, MnO_2 is also active as a catalyst for the conversion of $DPPH_2$ to DPPH. From preliminary experiments, the reproducibility of the reaction was the best with MnO_2, so this oxide

was chosen as representative catalyst for the mechanistic kinetic studies of the above conversion which are reported in the present paper. Suspensions of MnO_2 in organic liquids such as benzene are often mild, selective oxidants of organic compounds. For example, Gritter and Wallace (*4*) reported that unsaturated alcohols are more readily oxidized by MnO_2 than the corresponding saturated compounds. Thus EPR methods for the determination of the active oxygen surface area of MnO_2 catalysts should be of value in these oxidation reactions. Two such EPR procedures are discussed in this manuscript and the results obtained are compared with the corresponding data for the surface area of MnO_2 as measured by the conventional BET method. The principles of the two EPR methods outlined involve (i) reaction between $DPPH_2$ and MnO_2 and (ii) the direct adsorption of DPPH on MnO_2.

Experimental Methods

Reagents

Recrystallized benzene (May and Baker) was used without further purification as the solvent for $DPPH_2$ and DPPH. Manganese dioxide was prepared by the following reaction of permanganate with oxalic acid in neutral or alkaline solution. $KMnO_4$ (10.1 g) was dissolved in a minimum quantity of water and oxalic acid (12.9 g) in aqueous KOH so that the final pH was 10.5. The reagents were mixed and the pH was lowered to 7 by the gradual addition of 10 *N* HCl. The reaction appears to proceed very slowly at high pH. The precipitated MnO_2 was washed three times with water and acetone, then filtered in a glass crucible and dried over silica gel under low vacuum (water pump). Prior to use, this MnO_2 was heated at 120°C for 1.5 hr, then cooled in dry nitrogen.

$DPPH_2$ (Koch-Light) was recrystallized twice from a solvent mixture of ethanol and chloroform (3:2 v/v), the melting point (161–162°C, first recrystallization) rising to 175°C after the second recrystallization (174–176°C) (*5*). DPPH [Aldrich, or prepared from $DPPH_2$ with pre-reduced oxygen poisoned platinum (*3*)] was recrystallized from spectroscopic *n*-heptane, the melting point increasing from 119–121°C to 137–138°C after purification (Anal. calc.: C, 54.85%; H, 3.06%; found: C, 55.0%; H, 3.3%). DPPH should be kept in a desiccator at 20 ± 2°C, since, when exposed to air, a decrease in intensity of 10% for the same concentration in benzene can be observed after 1 month (samples degassed in intensity determinations). This effect is apparently due to the reaction of DPPH with water in the atmosphere.

(*i*) *Reaction Between $DPPH_2$ and MnO_2*

All reactions were performed in an evacuated H tube (Fig. 1a). DPPH concentrations were determined by electron paramagnetic resonance spectroscopy. For sample preparation, a known amount of oxide was placed in the thin part of the H tube. This part was long enough so that the oxide was outside the region of cavity absorption. This is necessary since the oxide tends to reduce the *Q* value of the cavity. An additional precaution to minimize the oxide effect during a particular run was taken by transferring most of the oxide, after the reactants had been mixed, to the large part of the H tube which originally contained the $DPPH_2$ solution. Further, the presence of MnO_2 in the cavity is undesirable because a superimposed spectrum of adsorbed and solution species might be obtained and MnO_2, being paramagnetic, can cause a slight drift in the base line.

For all experiments, the tubes were thoroughly dried at 125°C for 24 hr prior to use. For a particular run, the $DPPH_2$ solution was frozen in liquid nitrogen and the oxide was simultaneously cooled in Dry Ice/acetone while the system was evacuated to $\approx 5 \times 10^{-4}$ mm Hg. Cooling of the oxide was necessary to prevent "shooting" into the vacuum line.

The reactants were then mixed and, since the reaction is fast, the timing procedure in the actual EPR analysis was important. In all kinetic experiments, it was convenient to leave the chart paper running at 1 in./min for 30 min after the

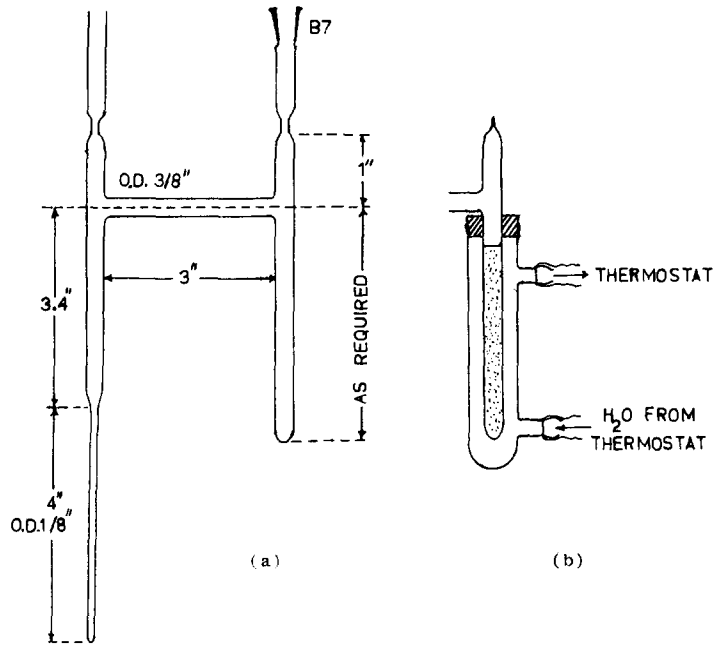

FIG. 1. (a) H tube for EPR surface area measurement; (b) Experimental arrangement for temperature dependence study of the $DPPH_2$-MnO_2 reaction.

mixing of reactants. The time of a particular peak was then determined by the distance of the central peak from the zero point. A fast scan was employed (100 G/min) and with practice, satisfactory spectra could be obtained at time intervals of 2 min. After each spectrum the tube was shaken thoroughly to minimize diffusion effects. It was not necessary to scan a complete spectrum, only the central peak of the conventional five line DPPH spectrum. Approximately 8–10 points could be obtained for the initial stages of the reaction. At this stage, which occurred approximately 20 min after the mixing of the reactants, the reaction was 80–90% completed as determined from the DPPH concentration.

After a particular reaction had reached a stationary concentration of DPPH, one end of the H tube was broken and the radical concentration was estimated in a calibrated silica EPR tube, after outgassing to 5×10^{-4} mm Hg. This determined concentration, C_{De}, can then be related to the intensity of the signal obtained in the H tube. If I_e is the intensity of the solution in the H tube, then intermediate nonstationary concentration values can be calculated from the relationship, $(I_t/I_e) \times C_{De}$, where I_t is the intensity at time t. All intensities were determined from the peak-to-peak height of the central line of the first derivative trace of DPPH. This estimate varies linearly with DPPH concentration up to approximately 2.5×10^{-3} moles liter^{-1} above which concentrations the line begins to assume a curvature with smaller slopes and thus above 2.5×10^{-3} moles liter^{-1} it is necessary to determine unknown concentrations from a calibrated curve.

(a) Effect of water. In order to study the effect of water on the reaction, the oxide was heated in an H tube at 120°C for 1.5 hr, then cooled in dry nitrogen. Water was then injected onto the walls of the "solution side" of the tube using a G.C. microsyringe (see Fig. 1a) and the tube stoppered (B7, thoroughly dried) using silicone grease. The MnO_2 was then immersed in Dry Ice/acetone, the wall of the tube was gently heated so that the water could be condensed onto the MnO_2 and the sys-

tem outgassed. Thorough drying of the tubes is necessary, otherwise adsorbed water on the glass walls will cause significant errors.

(b) Effect of temperature. In a study of the temperature dependence of the reaction, a satisfactory experimental procedure was developed using the equipment shown in Fig. 1b. While taking spectra, water was continually circulated from a thermostated bath. This procedure led to vibration of the sample in the cavity, resulting in some overall instability with some scatter of data. The effect of the vibration can be observed on the oscilloscope while "tuning" the instrument. The data were treated in the following manner. The intensities were plotted against time and the readings were taken from the curve to calculate concentrations. The error from benzene distilling over to the EPR side of the H tube (significant above 30°C) was ignored because of the slowness of the diffusion process. Finally, stationary concentrations were not affected by errors of this type, because determinations were performed independently in a calibrated tube.

(ii) Adsorption of DPPH

The studies of surface area measurement involving the direct adsorption of DPPH on MnO_2 were performed in an L-shaped tube (Fig. 2). A known amount of MnO_2 in the tube was heated at 120°C for 1.5 hr, cooled in dry nitrogen, a solution of known concentration of DPPH in benzene (5 ml) was added, and the stoppered tube was shaken for 20 min in a horizontal position. The tube was then inclined to allow sample withdrawal for EPR analysis. After the residual DPPH concentration was determined in a calibrated silica tube, the withdrawn sample was returned to the L tube. The calibrated silica tube was rinsed with benzene and this solvent used to dilute the sample in the L tube to give a different initial concentration of DPPH. Since part A of the tube was a burette, by noting the initial reading, the initial concentrations could be calculated and compared with those after adsorption.

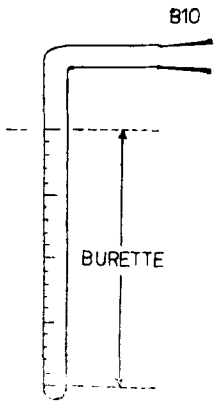

FIG. 2. L-shaped tube for DPPH adsorption studies.

EPR Instrument and Conditions

A Varian EPR spectrometer (V-4500) with 9-in. magnet and rectangular cavity was used. The modulation field was 0.48 G at 100 Hz throughout the experiments, except for the data in Fig. 8, where a value of 0.60 G was used.

Data Reproducibility

For MnO_2 prepared by the method outlined in the Reagents Section, batch-to-batch variations of $\pm 10\%$ can be observed. It is thus necessary to use a single batch of MnO_2 to be able to follow important trends in the mechanistic studies and this has been done in the present paper. A further problem with reproducibility is that although the data within a given set of experiments are reasonably consistent, the system does exhibit an occasional significant discrepancy when inter-set comparisons of data are made. For example, the values of C_{De} for 0.0120 and 0.0167 g of MnO_2 are 1.259 and 1.485×10^{-3} moles liter^{-1}, respectively (Table 2). These are not consistent with the result for 0.0156 g of MnO_2 for which $C_{De} = 1.100 \times 10^{-3}$ moles liter^{-1} (Table 3), and the difference in initial $DPPH_2$ concentration is not sufficient to explain this discrepancy. A plausible explanation can be found in the pretreatment of the sample. For each set of experiments, the MnO_2 samples in H tubes were subjected to the same treatment, by

TABLE 1
EFFECT OF VOLUME OF $DPPH_2$ SOLUTION ON DPPH CONVERSION FROM $DPPH_2$–MnO_2 REACTION[a]

Vol (ml)	$C_{De} \times 10^3$ (moles liter^{-1})	Slope $\times 10^2$ (min^{-1})	λ(moles^{-1} liters min^{-1})	N_{ap} ($\times 10^{-20}$)	Conversion (%)
5	1.560	8.43	100.6	3.09	65.1
10	1.025	8.47	61.6	4.04	42.8
15	0.780	8.60	53.1	4.69	32.6
20	0.618	8.48	47.6	4.84	25.8
35[b]	0.399	—	—	5.46	16.7
50[b]	0.294	—	—	5.83	12.3
75[b]	0.203	—	—	6.06	8.5

[a] Concentration of $DPPH_2$, 2.398×10^{-3} moles liter^{-1}, mass MnO_2, 0.0152 ± 0.0003 g; temp, 28°C.
[b] Only stationary concentration determined after 90 min; data obtained for constant m and C_0.

TABLE 2
EFFECT OF MASS OF MnO_2 ON DPPH CONVERSION FROM $DPPH_2$–MnO_2 REACTION[a]

Mass MnO_2 $\times 10^4$ (g)	$C_{De} \times 10^3$ (moles liter^{-1})	Slope $\times 10^2$ (min^{-1})	λ(moles^{-1} liter min^{-1})	N_{ap} ($\times 10^{-20}$)	Conversion (%)
462	1.972	8.50	94.0	2.57	68.6
374	1.866	8.55	84.6	3.00	64.9
344	1.832	8.55	81.9	3.21	63.7
316	1.800	8.53	79.4	3.43	62.6
289	1.765	8.58	77.2	3.68	61.4
250[b]	1.695	—	—	4.08	58.9
194	1.525	8.59	63.6	4.73	53.1
167	1.485	8.22	59.1	5.36	51.6
120	1.259	9.36	57.8	6.32	43.8
101	1.167	8.05	46.9	6.96[c]	40.6
91	1.140	7.46	43.0	7.55[c]	39.6
69	0.945	8.20	42.5	8.26[c]	32.8

[a] Concentration of $DPPH_2$ solution (10 ml of 2.876×10^{-3} moles liter^{-1}); temperature 28°C.
[b] Only stationary concentration determined after 90 min.
[c] The uncertainty in these results is high due to the relatively low masses of MnO_2 used.

TABLE 3
EFFECT OF INITIAL CONCENTRATION OF $DPPH_2$ ON DPPH CONVERSION IN $DPPH_2$–MnO_2 REACTION[a]

Mass MnO_2[b] $\times 10^4$ (g)	$C_0 \times 10^3$ (moles liter^{-1})	$C_{De} \times 10^3$ (moles liter^{-1})	Slope $\times 10^2$ (min^{-1})	λ(moles^{-1} liters min^{-1})	N_{ap} ($\times 10^{-20}$)	Conversion (%)
150	10.072	1.504	8.49	9.91	6.05	14.9
152	8.057	1.487	9.42	14.3	5.87	18.4
153	6.043	1.360	8.99	19.1	5.36	22.5
153	3.867	1.144	9.19	33.7	4.51	29.6
156	2.901	1.100	8.72	48.4	4.25	37.9
151	1.892	0.915	6.39	65.5	3.65	48.4

[a] Volume of solution, 10 ml; temp, 27°C.
[b] It will be observed that the values in this column are approximately constant at $\simeq 0.0153$ g.

TABLE 4
EFFECT OF ADDITION OF DDPH TO INITIAL SOLUTION OF $DPPH_2$ ON $DPPH_2$–MnO_2 REACTION[a]

$C_0 \times 10^3$ (moles liter^{-1})	C_{D0}[b] $\times 10^3$ (moles liter^{-1}) at $t = 0$	C_{De}[c] $\times 10^3$ (moles liter^{-1})	Slope $\times 10^2$ (min^{-1})	λ(moles^{-1} liter min^{-1})	$(C_{De} - C_{D0}) \times 10^3$ (mole liter^{-1})	Conversion (%)
2.388	0.155	0.931	10.46	64.4	0.776	32.5
2.418	0.345	1.029	11.35	64.7	0.684	28.3
2.408	0.600	1.295	8.49	49.6	0.695	28.9
2.418	0.946	0.980	6.86	28.8	0.034	1.4

[a] Volume of solution, 10 ml; temp, 19°C; mass of MnO_2 0.0237 ± 0.0003 g.
[b] C_{D0} = concentration of DPPH in initial solution of $DPPH_2$ at $t = 0$.
[c] C_{De} = total final concentration of DPPH including C_{D0}.

placing them in a temperature-controlled oven at the same time. Similarly, all were withdrawn at the same time to be cooled in a dry nitrogen atmosphere. After degassing, the H tubes were sealed off with the necessary $DPPH_2$ solution in the solution side of H tube as mentioned previously. Thus for each set of experiments all oxides were subjected to identical pretreatment conditions, of which temperature is particularly important. The time variation in oven temperature (thermocouple monitoring), where the MnO_2 was heated, was ±15°C. Further experiments have shown that with a more accurate control (±3°C) the above isolated discrepancies can be eliminated.

In summary, eight sets of experiments were carried out in the present investigation: (a) volume of $DPPH_2$ solution varied; (b) mass of MnO_2 varied; (c) initial concentration of $DPPH_2$ varied; (d) addition of DPPH to the initial $DPPH_2$ solution; (e) effect of water; (f) effect of temperature; (g) the oxide before and after reaction; (h) DPPH adsorption studies. These surface area results were then compared with conventional nitrogen BET determinations.

RESULTS

Surface Area from Reaction Between $DPPH_2$ and MNO_2

All data are summarized in Tables 1–7 and Figs. 3–15. The kinetic data for the reaction between $DPPH_2$ and MnO_2 (e.g., Figs. 3 and 4) were found to obey Eq. (1) for 20 to 30 min of the reaction* where C_0 is the initial concentration of $DPPH_2$, C_{De} is the stationary state concentration of DPPH, C_D is the instantaneous concentration of DPPH at time t and λ and I are constants. The slope of the graph of

$$\frac{1}{C_0 - C_{De}} \ln \frac{C_0 - C_D}{C_{De} - C_D} = \lambda t + I, \quad (1)$$

* This corresponds to ~80 to 90% of the stationary concentration value (i.e., C_D/C_{De} ~0.8 to 0.9).

TABLE 5
REACTIVITIES OF USED AND UNUSED OXIDE IN THE MnO_2–$DPPH_2$ REACTION[a]

	Mass $\times 10^4$ (g)	Slope $\times 10^2$ (min^{-1})	λ (moles^{-1} liter min^{-1})	$C_{De} \times 10^3$ (moles liter^{-1})
(1) MnO_2, fresh	299	8.09	73.8	1.780
(2) Used MnO_2 [from reaction(1)]	108	6.54	25.1	0.269

[a] Temp, 23°C; $C_0 = 2.876 \times 10^{-3}$ moles liter^{-1}; $DPPH_2$ solution = 10 ml.

TABLE 6
EFFECT OF WATER ON $DPPH_2$–MnO_2 REACTION[a]

Set A[b]					Set B[b]				
t_e[c] (min)	H_2O (μl)	$C_{De} \times 10^3$ (moles liter^{-1})	Slope $\times 10^2$ (min^{-1})	λ(moles^{-1} liters min^{-1})	t_e[c] (min)	H_2O (μl)	$C_{De} \times 10^3$ (moles liter^{-1})	Slope $\times 10^2$ (min^{-1})	λ (moles^{-1} liter min^{-1})
47	0	0.901	7.46	48.6	55	0	1.100	7.28	54.5
49	6.0	0.875	8.48	54.4	75	2.5	1.064	7.30	53.5
85	10.0	0.791	5.83	35.5	85	5.0	1.022	6.92	48.9
230	15.0	0.719	2.09	12.2	90	7.5	0.977	6.46	44.3
255	25.0	0.616	1.09	6.0		15.0[d]	0.850	—	—
					300	30.0	0.603	0.78	4.26

[a] $DPPH_2$ solution (10 ml of 2.436×10^{-3} moles liter^{-1}); temp, 19°C; MnO_2 0.0154 ± 0.0003 g.
[b] Division of experimental results into two sets is not an experimental one, but is based on the data which show two distinct lines for C_{De} vs μl of H_2O (Fig. 9).
[c] t_e is time required to attain steady state.
[d] Only stationary concentration observed after 5 hr.

$\ln(C_0 - C_D)/(C_{De} - C_D)$ vs t is defined by an additional parameter S [Eq. (2)].

$$\lambda = \frac{S}{C_0 - C_{De}}. \tag{2}$$

The apparent number of active sites, N_{ap}, on the oxide where reaction occurs will be defined by Eq. (3)

$$N_{ap} = \frac{VC_{De}}{m} N_0, \tag{3}$$

where V is the volume of $DPPH_2$ solution in liters, m, the mass of the oxide in grams and N_0, Avogadro's number. The percentage conversion (Y) of $DPPH_2$ into DPPH is calculated by assuming that the residual adsorption of DPPH on the surface is insignificant under the experimental conditions used. Data are presented below to support this conclusion.

The effect of volume of $DPPH_2$ solution on C_{De}, λ, N_{ap} and Y is shown in Table 1. The relevant kinetic graphs are shown in Fig. 3 while in Fig. 4 these data are plotted according to Eq. (1) at constant values of m and C_0. Table 2 and Fig. 5 summarize the effect of mass of oxide on the reaction at constant V and C_0, while the dependence of C_{De}, S, λ, N_{ap}, and Y on the initial concentration of $DPPH_2$ at constant m and V is shown in Table 3. The poisoning effect of DPPH is illustrated by Table 4 where both λ and $(C_{De} - C_{D0})$ indicate that poisoning becomes significant at $C_{D0} > 0.6 \times 10^{-3}$ moles/liter^{-1}, C_{D0} being the concentration of DPPH in the initial solution of $DPPH_2$ (at $t = 0$).

The effect of V, m and C_0 on N_{ap} is shown in Fig. 6 while in Fig. 7, λ is shown as a function of V, m, C_0, and C_{D0}. It should be

TABLE 7
EFFECT OF TEMPERATURE ON $DPPH_2$–MnO_2 REACTION[a]

T (°K)	$C_{De} \times 10^3$ (moles liter^{-1})	$\frac{1}{T} \times 10^3$	Slope $\times 10^2$ (min^{-1})	λ (moles^{-1} liter min^{-1})	$\log_{10} \lambda$
298	0.860	3.356	5.34	34.8	1.541
303	0.916	3.300	5.80	39.3	1.594
308	0.869	3.247	7.41	48.6	1.687
318	1.030	3.145	8.09	59.4	1.773
323	0.926	3.095	9.68	66.0	1.820

[a] Concentration of $DPPH_2$ solution (10 ml of 2.392×10^{-3} mole liter^{-1}); MnO_2 0.0153 ± 0.0003 g.

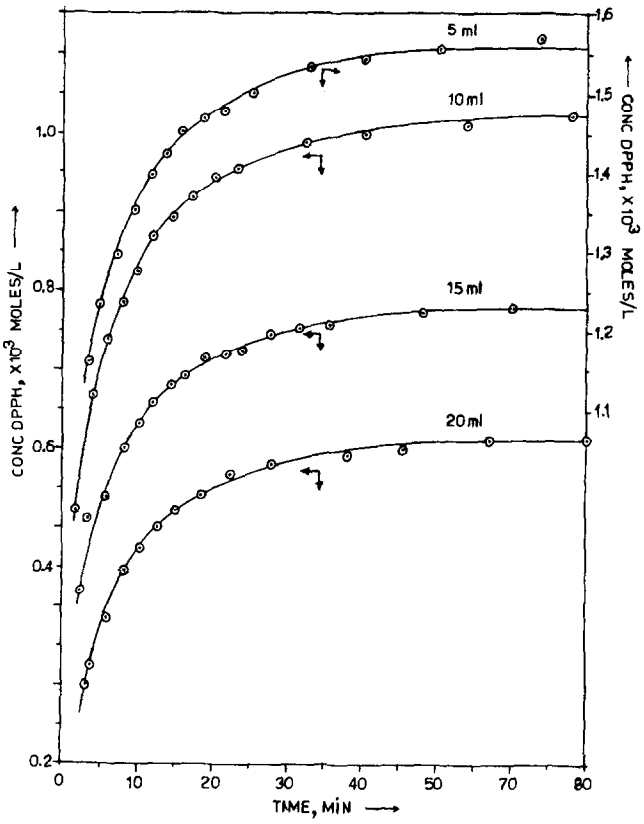

FIG. 3. Kinetic curves for volume variation experiments. Concentration of DPPH produced vs time; temp, 28°C; $C_0 = 2.398 \times 10^{-3}$ moles liter^{-1}; $MnO_2 = 0.0152 \pm 0.0003$ g.

noted that λ is a linear function of m and $1/V$, and that theoretically the curve N_{ap} vs m should pass through the origin. There are indications that the curve passes through a maximum between 0 and 10 mg of oxide; however, scatter of data in this region precludes any definite conclusions. The relatively poor reproducibility for those experiments where the mass of oxide is reduced may be due to enhancement of differences in properties such as particle size, surface area, and accidental uptake of water within a batch. The system is particularly susceptible to water as the subsequent discussion shows. Evidence for the degree of scatter in the low mass region is shown in Fig. 6.

The effect of residual DPPH adsorption on the activity of the oxide for the $DPPH_2$–MnO_2 reaction is shown in Table 5. Experiments were performed on a batch of *used* MnO_2 which had been rinsed four times with benzene and evacuated to 5×10^{-4} mm Hg for 0.5 hr before being reacted again. The EPR spectra of the oxides prior to and after reaction with $DPPH_2$ are shown in Fig. 8. The arrow in the top spectrum denotes the resonance position of polycrystalline DPPH and was determined by obtaining a spectrum of unused MnO_2 simultaneously with DPPH. In the lower spectrum a narrow signal at the g value of polycrystalline DPPH [$g = 2.0036$ (*6*)] is shown superimposed on the resonance of the used MnO_2. Since the used oxide was rinsed with benzene until no resonance of DPPH could be detected in the solvent, the above result indicates that DPPH is chemisorbed on some sites on the surface. It also provides evidence to support the existence of a stationary concentration of DPPH in the system.

(a) Effect of water on reaction. Water is found to inhibit the conversion of

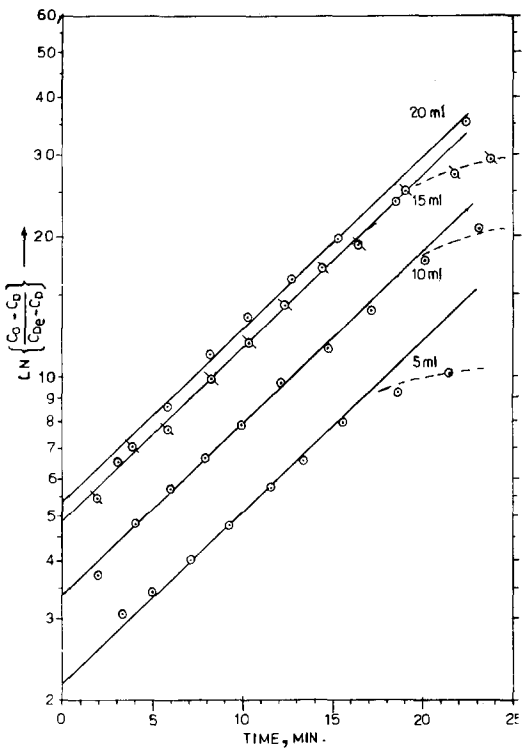

FIG. 4. Graph of $\ln(C_0 - C_D)/(C_{De} - C_D)$ vs time for the volume variation experiments.

$DPPH_2$ into DPPH (Table 6),* the results being plotted in Fig. 9 where the linearity between C_{De} and μl of H_2O should be noted. Typical kinetic curves for differing amounts of water are shown in Fig. 10 while in Fig. 11 the data have been plotted according to the relationship of Eq. (1). In the initial stages of the reaction, it is observed that $\ln(C_0 - C_D)/(C_{De} - C_D)$ is still a linear function of t (cf. Fig. 4), the values of the parameter λ being deduced from these initial points. With the exception of C_{De} which was determined in a calibrated tube, the data in later parts of the curve were significantly less reproducible. With increasing quantities of water, the time required to reach a stationary concentration was delayed and the data were too scattered for further evaluation. The effect of water on the empirical rate constant (λ) is shown in Fig. 12.

(b) Effect of temperature on reaction. As before, the data were treated by plotting intensities against time, a typical plot being shown in Fig. 13. By comparison with the other kinetic curves (e.g., Fig. 3), the points at higher temperatures are much more scattered. The results for five different temperatures are summarized in Table 7, the corresponding Arrhenius plot (Fig. 14) giving an apparent activation energy (E_a) of 5.1 kcal mole^{-1} and a frequency factor (A) of 1.84×10^5 moles^{-1} liter min^{-1}.

Surface Area from DPPH Adsorption on MnO_2

In this second method for surface area determination by measuring the direct adsorption of DPPH onto the oxide, the same batch of MnO_2 was used as in the preceding series of experiments. The results are shown in Fig. 15 where the adsorbed DPPH (g/g of oxide) is plotted against initial DPPH concentration. For the experiment, MnO_2 (0.1034 g) was used with an initial DPPH concentration before dilution of 6.50×10^{-3} moles liter^{-1}.

Discussion

Surface Area from Reaction Between $DPPH_2$ and MnO_2

Elementary considerations suggest that the reaction rate should depend on the concentration of $DPPH_2$ and the number of active sites of MnO_2 (i.e., not yet consumed) on the surface. If the rate-controlling step is diffusion of $DPPH_2$ to the surface where reaction occurs, then it can be shown that the data should follow Eq. (4) where C_0 is the initial concentration of $DPPH_2$, C_t, the instantaneous concentration of $DPPH_2$ at time t, A, the surface area, V, the volume of solution, k, the rate constant of the surface reaction, δ, the

$$\ln \frac{C_0}{C_t} = \frac{A}{V}\left(\frac{1}{(\delta/D) + (1/k)}\right)t \qquad (4)$$

* The experimental results have been divided into two groups based on the data which show two distinct lines for C_{De} vs μl of H_2O. The referee prefers to accept the scatter of the relevant data and to draw a single line in Fig. 9. This is a valid suggestion; however, the authors prefer to leave the original format since the results may reflect a site effect in the catalyst.

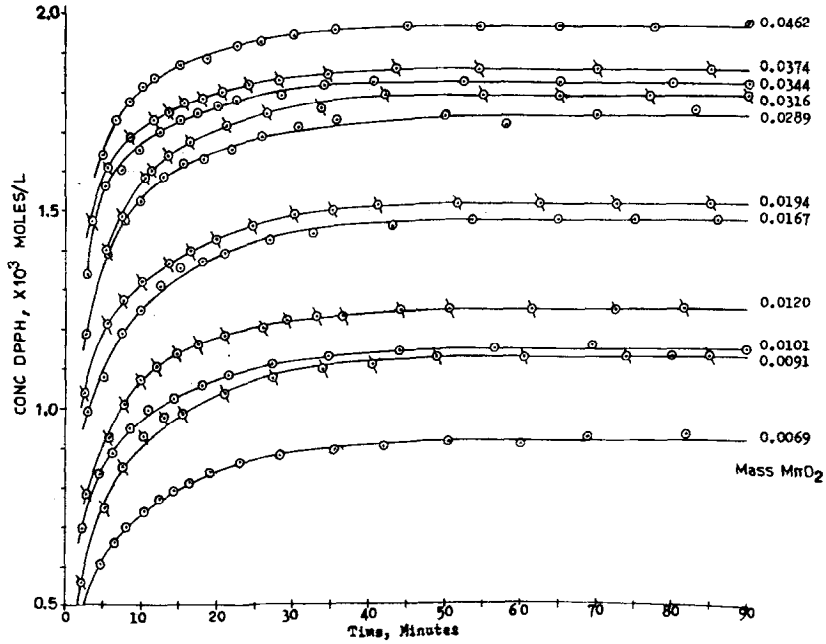

FIG. 5. Kinetic curves for mass variation experiments: temp, 28°C; $C_0 = 2.876 \times 10^{-3}$ moles liter^{-1}; volume of solution = 10 ml.

thickness of the diffusion layer and D, the diffusion coefficient (7). The data however, follow Eq. (1) which is comparable to the second order integrated Eq. (5). The data also obey Eq. (1) for 20–30 min of the reaction, this corresponding to ~ 80 to 90% of the stationary concentration value (i.e., $C_D/C_{De} \sim 0.8$ to 0.9). Under these conditions Eq. (6) represents the differential equation for the reaction and corre-

$$\frac{1}{a-b} \ln \frac{b(a-x)}{a(b-x)} = kt, \qquad (5)$$

$$\frac{dC_D}{dt} = \lambda(C_0 - C_D)(C_{De} - C_D) \qquad (6)$$

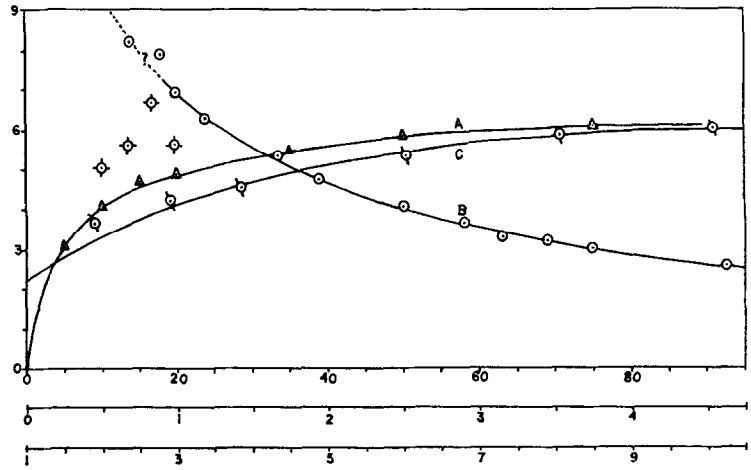

FIG. 6. Apparent number of active sites (N_{ap}) vs volume of solution (A), mass of MnO_2 (B), and initial concentration (C_0) (C). Note that between 0–10 mg of MnO_2, data show bad scatter. Also observe the points denoted by ⊕ for which only the stationary concentration of DPPH were determined. These are not shown in Table 2.

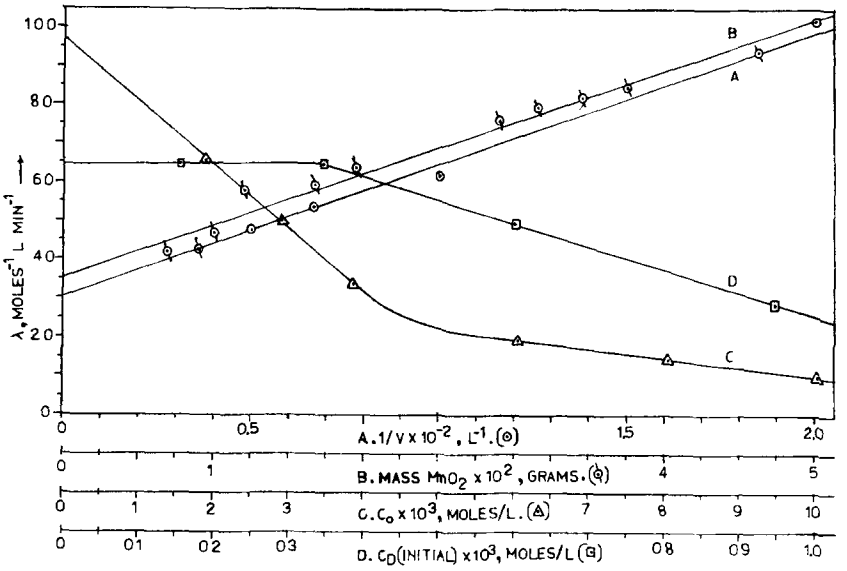

FIG. 7. Empirical rate constant (λ) as a function of $(\text{vol})^{-1}$, mass MnO_2, initial $DPPH_2$ concentration (C_0) and initial DPPH concentration (C_{D_0}).

sponds in format to conventional Eq. (7). However, this equation represents an extremely simple case and the comparison is only of limited applicability.

$$\frac{dx}{dt} = k(a - x)(b - x) \tag{7}$$

The constant I [Eq. (8)] can be evaluated at $t = 0$ in Eq. (1).

$$I = \frac{1}{C_0 - C_{D_0}} \ln \frac{C_0}{C_{De}} \tag{8}$$

Thus a graph of $\ln(C_0 - C_D)/(C_{De} - C_D)$ vs t should have an intercept of $\ln C_0/C_{De}$. Despite the apparently regular variation of the intercept with respect to volume in Fig. 4, the values for this parameter tend to be very scattered in other experiments, particularly for the mass variation experiment. Furthermore, for certain of the experiments (e.g., mass variation), the value of the intercept is invariably greater than predicted. A plausible explanation for this

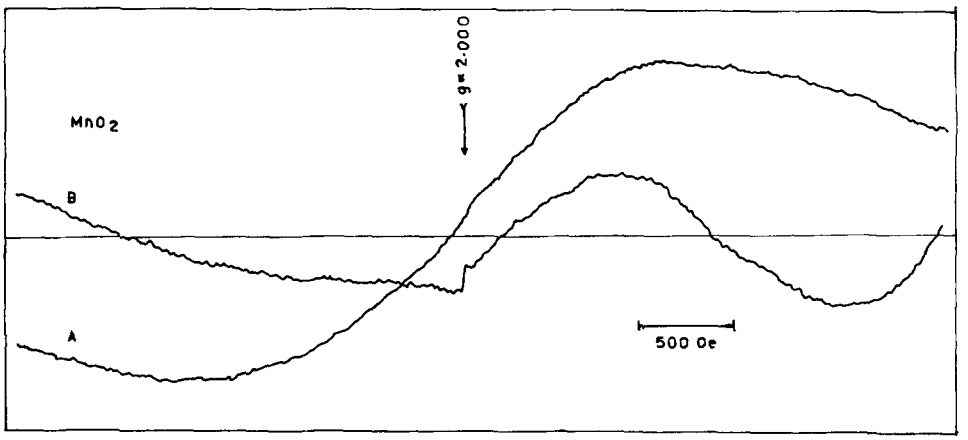

FIG. 8. EPR spectra of (A) fresh, and (B) used MnO_2. The weak narrow signal superimposed on the resonance of the used oxide indicates an adsorbed radical species, presumably DPPH.

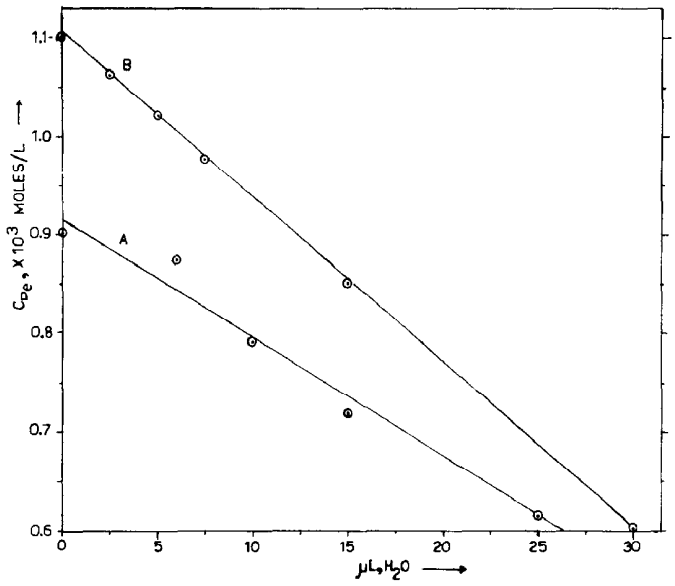

FIG. 9. Stationary concentration of DPPH (C_{D_0}) vs μl of H_2O on the oxide.

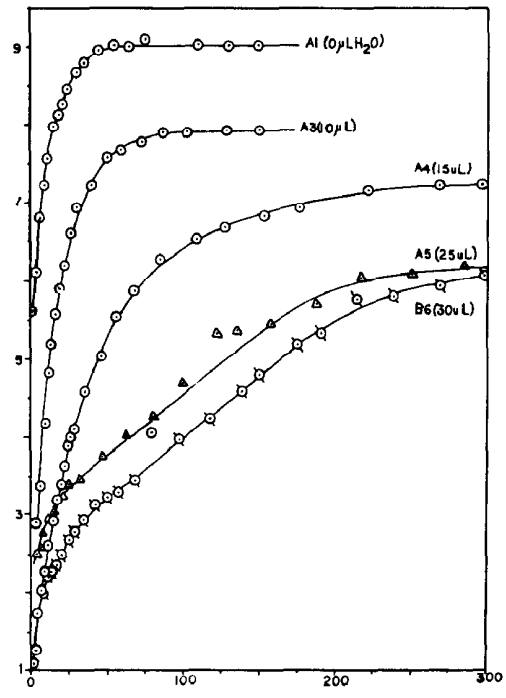

FIG. 10. Kinetic curves illustrating the effect of water on the concentration of DPPH produced (C_D) vs time: temp, 19°C; mass MnO_2 = 0.0154 ± 0.0003 g; C_0 = 2.436 × 10^{-3} moles liter^{-1}; volume of solution = 10 ml.

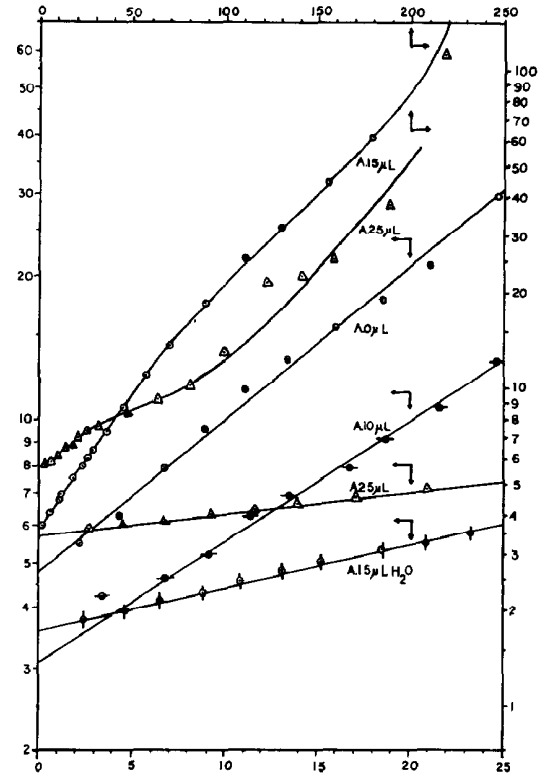

FIG. 11. Effect of water on $\ln(C_D - C_D)/(C_{D_0} - C_D)$ vs time. The letters A and B refer to sets A and B of Table 6.

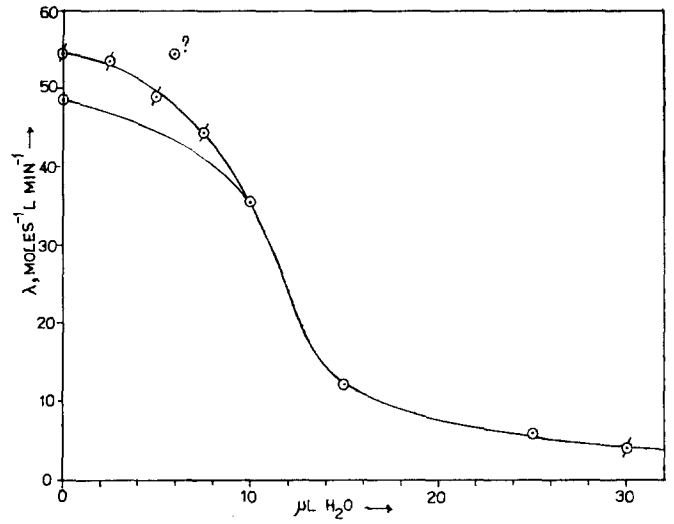

FIG. 12. Effect of water on the empirical rate constant (λ).

difference involves the presence of very active sites for the abstraction of hydrogen from $DPPH_2$. Thus, if some sites are extremely active, some $DPPH_2$ would already have been converted to DPPH at $t = 0$. This suggestion is substantiated by the fact that most of the kinetic curves do not pass through the origin.

Evidence suggesting a reaction involving the formation of a stationary concentration of DPPH is shown in Tables 1–3 and Fig. 6. In the volume variation experiment, C_{De} decreases and N_{ap} increases with increasing volume. As the mass of MnO_2 is increased, C_{De} increases but N_{ap} decreases. All these changes occur asymptotically and can be interpreted in terms of DPPH adsorption. For example, with an increase in volume of reagent solution for a constant mass of MnO_2, the DPPH concentration will be

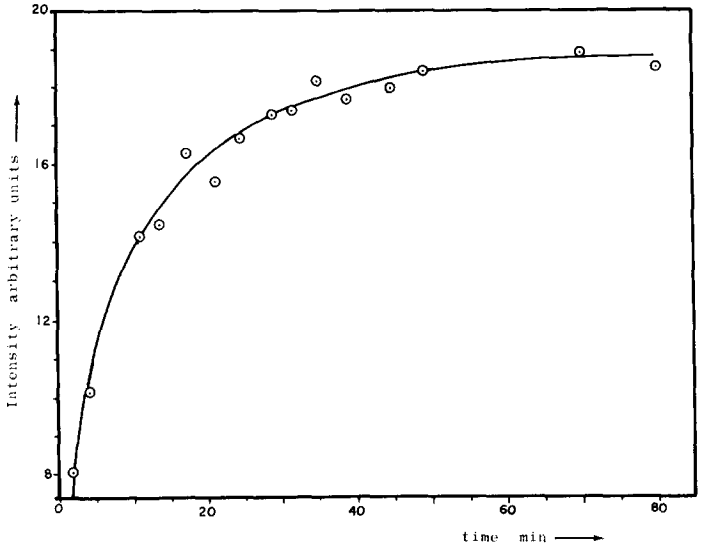

FIG. 13. Typical graph of intensity vs time in temperature studies: Example shows the curve for T = 308°K (see Table 7).

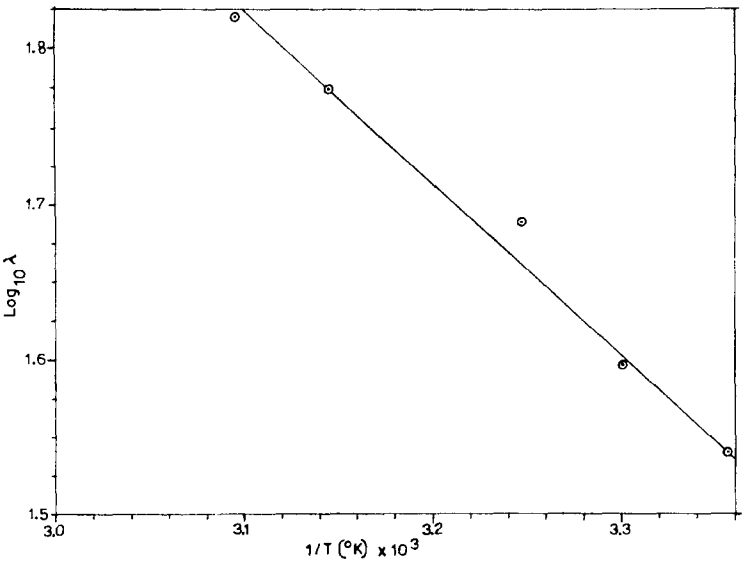

FIG. 14. Arrhenius plot of $\log_{10}\lambda$ vs $(1/T)$.

decreased and the extent of adsorption of this molecular species will be reduced. Alternatively, if the mass of MnO_2 is increased, two effects may be observed. Firstly, the concentration of DPPH should increase due to the increase in number of active sites available for hydrogen abstraction. Secondly, despite the increase in active sites, there should be a corresponding increase in surface area and DPPH adsorption will become more significant. The data suggest that DPPH adsorption is a limiting factor in the conversion of $DPPH_2$, e.g., in Table 4 where the effect of DPPH on the initial $DPPH_2$ solution was investigated. From the percentage conversion, it would appear that DPPH poisons the reaction by covering the active sites on the surface. The effect is only significant if the concentration of DPPH is above 0.6×10^{-3} moles $liter^{-1}$ for $\sim$0.02 g of MnO_2 and implies that DPPH is preferentially adsorbed when compared with $DPPH_2$ above this critical concentration. These results also suggest that $DPPH_2$ adsorbs by charge–transfer bonding (*8*) through both

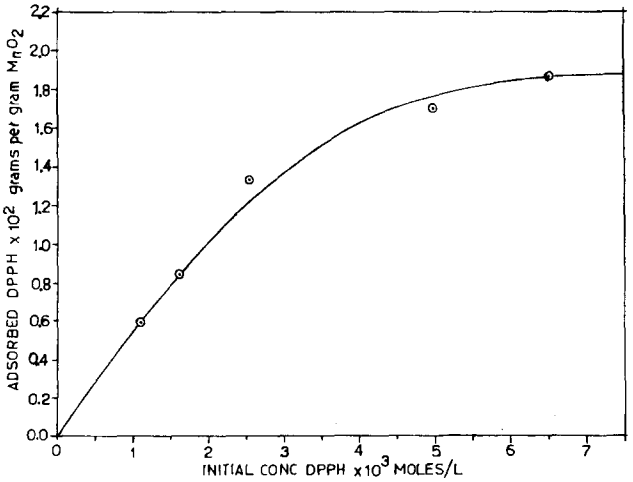

FIG. 15. Adsorption of DPPH on MnO_2 vs initial DPPH concentration: temp, 19°C.

the π-electrons of the aromatic rings and the lone-pair on the nitrogen atoms, whereas DPPH may be more strongly adsorbed presumably through σ-bonded species involving interaction with the unpaired electron. This interpretation is consistent with studies of relative adsorption strengths of aromatic compounds on catalytic surfaces in isotope exchange and hydrogenation reactions (*8*) where radical species such as DPPH are strongly adsorbed (compared with compounds such as $DPPH_2$) and lead to significant reagent displacement effects in the catalytic reaction. However, the present system is more complicated than the simple exchange example since in the DPPH work additional species are present in the reagent solution and on the surface of the catalyst, thus leading to the possibility of competing surface reactions occurring at relatively high initial DPPH concentrations. This suggestion would explain the observed maximum in the final (total) concentration of DPPH in Table 4.

An additional indicator of the effect of DPPH is provided by λ. Below initial DPPH concentrations of 0.345×10^{-3} moles liter^{-1}, λ remains virtually constant ($\sim$64.4) while at higher concentrations, λ decreases linearly (Fig. 7). Moreover, the data in Table 3 suggest that after hydrogen abstraction from charge–transfer adsorbed $DPPH_2$, the DPPH formed will be liberated in solution, leaving OH at the surface site. DPPH may then be readsorbed as a σ-bonded species at some other site, the probability of this readsorption process decreasing as the $DPPH_2$ concentration is increased (Fig. 7).

If a steady state exists in the system, the used oxide after reaction should still be capable of abstracting hydrogen from $DPPH_2$. Such evidence is provided in Table 5 where the used MnO_2 was rinsed four times with benzene and evacuated on the vacuum line prior to being reacted again. For the used oxide, the values of λ (25.1 moles^{-1} liters min^{-1}) and C_{De} (0.269×10^{-3} moles liter^{-1}) are considerably lower than the corresponding values obtained for the same mass of unused oxide (46.9 and 1.167×10^{-3}, respectively). It is also to be noted that λ from the used oxide is even smaller than the constant 35.6 obtained by extrapolating λ to zero mass (Fig. 7). It thus appears that MnO_2 undergoes considerable changes during the reaction and this conclusion is confirmed from the EPR spectra of used and unused MnO_2 (Fig. 8). These spectra are different, indicating that either the crystal structure has been modified significantly or the change in the surface due to reaction is transmitted and has a magnetic effect on the manganese atoms, i.e., it alters the magnetic environment of the manganese atoms responsible for the observed paramagnetism. Furthermore, a signal of small width was observed at the g value of polycrystalline DPPH, thus indicating the presence of an adsorbed radical species which almost certainly was DPPH.

The slope of the graph of $\ln(C_0 - C_D)/(C_{De} - C_D)$ vs t (Fig. 4) is remarkably constant ($S \sim 8.50 \times 10^2$ min^{-1}). However, λ varies significantly and regularly and is a linear function of V^{-1} [Eq. (9)] and m [Eq. (10)], the relevant data being plotted in Fig. 7.

$$\lambda = 0.34(V^{-1}) + 30.6, \qquad (9)$$

$$\lambda = 1332m + 35.6. \qquad (10)$$

The first relationship was obtained for constant values of m (0.0152 g) and C_0 (2.398×10^{-3} moles liter^{-1}) while the second was deduced for constant V (10 ml) and C_0 (2.876×10^{-3} moles liter^{-1}). Attempts to formulate a mechanism to explain the constants 30.6 and 35.6 moles^{-1} liters min^{-1} have been unsuccessful. Diffusion processes are obviously important in these reactions in spite of the vigorous shaking since the apparent activation energy of 5.1 kcal mole^{-1} (Fig. 14) is within the range of 3.00 to 7.00 kcal mole^{-1} (*9*) expected for diffusion controlled reactions.

The decrease in λ with increasing C_0 can be explained by considering the relationship in Eq. (2). From this expression and since C_{De} and N_{ap} increase asymptotically with C_0, λ will decrease with increasing C_0. Thus, under these conditions, λ can no

longer be regarded as a rate constant due to the large excess of C_0.

(a) Effect of water on reaction. Water reduces the stationary concentration of DPPH (Table 6 and Fig. 9) and distorts the kinetic curve (Fig. 10). This curve distortion is significant and may be used as a qualitative test for the presence of significant amounts of water. Normally the stationary concentration of DPPH is reached in 20–30 min, however water retards the reaction and the stationary concentration is not attained until after 4–6 hr (Fig. 10), an effect which is noticeable only if the amount of water introduced exceeds 10 μl. These observations can be interpreted in terms of displacement of water by $DPPH_2$, such a process becoming more difficult as the quantity of water on the surface increases. Again unequivocal evidence for competition between water and an aromatic reagent for a catalyst site is found in isotope exchange reactions on Group VIII transition metals and their oxides (*8*). A similar type of process is envisaged in the $DPPH_2$ system. In addition, the reverse reaction becomes more probable as the proton concentration on the surface increases. In an analogous system, the reaction of surface water on TiO_2 with DPPH yields $DPPH_2$ as the main product with considerable quantities of *p*-benzoquinone and some 2′,4′,6′-trinitro-4-aminodiphenylamine (*10, 11*). In the present MnO_2 studies, thin-layer chromatography has detected only DPPH and $DPPH_2$. It should be pointed out that in the TiO_2 work, a monolayer of sulfuric acid was on the surface of the oxide.

Figure 9 shows that the stationary concentration of DPPH, C_{De}, decreases linearly with the amount of water introduced into the system. Extrapolation to $C_{De} = 0$ gives 65.9 and 76.3 μl of H_2O for 0.0154 g of MnO_2, thus the reaction does not proceed when ~71 μl of H_2O covers the surface. Theoretically, λ should be zero at the cut-off water coverage; however, in practice such a determination is inaccurate due to the nonlinearity of λ with respect to the amount of water on the surface (Fig. 12).

(b) Reaction mechanism. A plausible reaction mechanism consistent with the data involves the charge–transfer adsorption of $DPPH_2$ on the surface followed by hydrogen abstraction to give DPPH and adsorbed hydroxyl radicals. In this respect, lattice oxygen in oxides such as MnO_2 is considered to have a mobile character and thus is important in determining the rate of the reaction. The sequence of events may be represented by the following four equations:

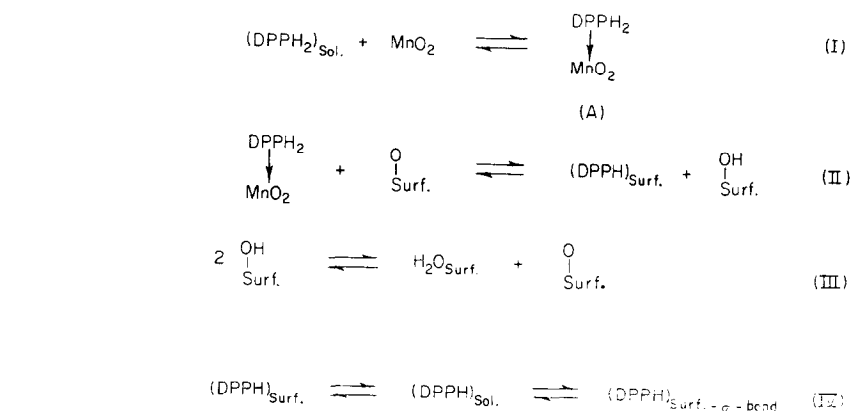

From previous EPR work involving adsorption of aromatic compounds on inorganic oxides (*12–14*), the charge–transfer complex between the surface and $DPPH_2$ most probably involves the Mn^{4+} atoms and one of the phenyl rings. From molecular models it is clear that one of the phenyl rings can easily interact with a surface and in such a complex the hydrogen

of the hydrazine group is near the surface, i.e., initial π-complex formation through the phenyl rings lowers the activation energy associated with N–H bond rupture. A similar observation has been made for the adsorption of alkylbenzenes through their alkyl groups on certain metals and metal oxides (*8*). Further, a similar type of complex to that in [Eq. (I)] has been postulated in the oxidation of *trans*-cinnamyl alcohol to the corresponding aldehyde by MnO_2 suspension in ether (*15*). The proposed charge–transfer species [(A) in Eq. (I)] is consistent with the analysis of Dunitz and Orgel (*16*) who showed that σ- or π-binding between metal ions (such as Mn^{4+}) and unsaturated hydrocarbons can occur.

The charge–transfer adsorption step is followed by hydrogen abstraction to give adsorbed hydroxyl radicals [Eq. (II)]. These may then disproportionate [Eq. (III)] to water and atomic oxygen which is then scavenged by reaction with additional $DPPH_2$. This proposed sequence of reaction steps is based on current knowledge of π-complex formation in heterogeneous catalysis, however, the exact mechanism for the interaction of $DPPH_2$ with MnO_2, particularly for the hydrogen abstraction step, cannot be further refined at this time without additional work. In particular, a complete mathematical formulation of the reaction does not yet seem feasible due to the complexity of the system. The Langmuir approach* to the problem has been considered but is not completely satisfactory. Nevertheless, the proposed mechanism does explain the major features of the reaction.

(c) Actual active surface area determination—$DPPH_2$ with MnO_2. It has been shown that N_{ap} increases asymptotically with increasing V and C_0, both curves tending toward a value of 6.1×10^{20} (Fig. 6). If it is assumed that this figure† represents the number of active oxygen atoms per gram of MnO_2 capable of abstracting hydrogen from $DPPH_2$ to yield DPPH, this concept can be used as a plausible basis for active surface area determination. Using a value for van der Waals radius of oxygen of 1.40 Å (*17*) and, assuming hexagonal close packing of spheres on the surface, the effective area of an oxygen atom will be $2\sqrt{3} \times 1.40^2$ or 6.8 Å^2. From this value, a surface area of 41.5 m^2/g of MnO_2 is obtained. If instead, the active species on the surface is considered to be O^{2-}, for which there is some evidence (*18*), then from Slater's estimate (*19*) of 1.45 Å for the ionic radius of this species, a surface area of 44.5 m^2/g of MnO_2 is deduced.

Surface Area from DPPH Adsorption

The adsorption of DPPH on solid surfaces has been studied extensively (*10, 11, 20–23*). It has been shown (*24*) that in the range from 0.02 to 0.10 degrees of surface coverage, the adsorbed DPPH exists in a state of molecular aggregates on silica gel, aluminum gel, barium sulfate and zinc oxide. X-ray diffraction (*25*) has revealed that the molecule is not planar in a single crystal of DPPH containing benzene. However, from EPR studies, Lord and Blinder (*26*) concluded that DPPH is essentially planar in dilute solutions. Misra (*21*) deduced a radius of 6.80 Å for the molecule and used this value to calculate the surface area of carbon black from adsorption studies of DPPH. Assuming hexagonal close packing of spheres on the surface, it can be shown that the effective area of a DPPH molecule is $2\sqrt{3}\ r^2$ or 160.18 Å^2. Using this value, Misra obtained a surface area of 198.5 m^2/g which was, significantly, equal to his electron micrographic area of 200 m^2/g.

* Reaction rate α [$DPPH_2$], fraction of active sites of MnO_2 *not yet* consumed α [$DPPH_2$] $(1 - \theta)$.

† It might appear from the mass variation experiment (Table 2, Fig. 6) that N_{ap} could be at least 8.26×10^{20}; however, at low masses, particularly for the region of 10 mg and below, the data exhibit bad scatter (Fig. 6) and thus a reliable N_{ap} value on this basis cannot be obtained. Because of the small masses of oxide involved in this region, the scatter seems to be due predominantly to the unavoidable pickup of traces of moisture during handling and this source of error is accentuated at very low oxide masses.

The adsorption of DPPH on MnO_2 as a function of initial DPPH concentration is shown in Fig. 15. From this graph, a saturation coverage of 1.88×10^{-2} g of DPPH/g MnO_2 is deduced. This means that the surface area of the oxide is $1.88 \times 10^{-2} \times (394)^{-1} \times 6.024 \times 10^{23} \times 160.18^2$ or 46 m^2/g, which compares very favorably with the value obtained from the active oxygen method. In the above adsorption experiment, 0.1034 g of MnO_2 was used. In most of the experiments performed, adsorption will be relatively insignificant in terms of concentration changes. For example, at an initial concentration of 1.100×10^{-3} moles $liter^{-1}$, the decrease in concentration is 0.07×10^{-3} moles $liter^{-1}$, thus for 0.0155 g, the decrease in concentration would be 0.01×10^{-3} moles $liter^{-1}$. The EPR value of 46 m^2/g is to be compared with a BET value of 61 m^2/g and accentuates the fact that EPR methods determine essentially the active surface area as distinct from surface area measurements which are obtained by physical adsorption techniques (*27*).

Conclusions

Kinetic data show that the reaction between $DPPH_2$ and MnO_2 produces a stationary concentration of DPPH. The results suggest that DPPH adsorption on the surface is the limiting factor in the reaction, this effect being significant for concentrations of DPPH above 0.6×10^{-3} moles $liter^{-1}$ for 23.7 mg of MnO_2. Because of its large size, the adsorption of one molecule of DPPH means that approximately 24 active oxygen atoms will be covered (assuming hexagonal close packing of both DPPH and active oxygen and taking 160.18 and 6.80 $Å^2$ for the effective areas of DPPH and oxygen, respectively). This view is substantiated by the fact that DPPH addition to the initial solution of $DPPH_2$ in benzene inhibits the reaction.

The $DPPH_2$–MnO_2 reaction obeys the empirical Eq. (1). The apparent activation energy is 5.1 kcal $mole^{-1}$ and the frequency factor 1.84×10^5 $moles^{-1}$ liters min^{-1}. It is probable that diffusion processes play an important role in the reaction. Water reduces the value of C_{De} and the λ parameter. The former decreases linearly with increasing water coverage on the surface.

Two consistent estimates of the surface area of active sites in MnO_2 (61 m^2/g by BET) have been obtained by determinations of active oxygen (41.5 m^2/g) and DPPH adsorption (46 m^2/g). In these calculations, hexagonal close packing is assumed. The consistency of the results is significant. Batch-to-batch reproducibility of the oxide was generally $\pm 10\%$. In the experiments described, a single batch was used.

Acknowledgments

The authors thank both the donors of the Petroleum Research Fund administered by the American Chemical Society and the Australian Research Grants Committee for the support of this research. One of us (A. T. T. O.) wishes to express his gratitude to the Australian Department of Science and Education for a fellowship. The authors are also grateful to K. Catchpole for assistance with the BET measurements.

References

1. Goldschmidt, S., and Renn, K., *Chem. Ber.* **55,** 636 (1922).
2. Kuhn, R., and Manner, I., *Chem. Ber.* **83,** 413 (1950).
3. Garnett, J. L., Oei, A. T. T., and Sollich-Baumgartner, W. A., *J. Catal.* **7,** 305 (1967).
4. Gritter, R. J., and Wallace, T. J., *J. Org. Chem.* **24,** 1051 (1959).
5. Poirier, R. H., Kahler, E. J., and Benington, F., *J. Org. Chem.* **17,** 1437 (1952).
6. Holden, A. N., Kittel, C., Merrit, R. F., and Yager, W. A., *Phys. Rev.* **77,** 147 (1950).
7. Lee, T. S., "Techniques of Organic Chemistry" (A. Weissberger, ed.), Vol. 8, p. 127. Interscience, New York, 1953.
8. Garnett, J. L., and Sollich-Baumgartner, W. A., *Advan. Catal. Relat. Subj.* **16,** 95 (1966).
9. Benson, S. W., "The Foundation of Chemical Kinetics," pp. 496–502. McGraw-Hill, New York, 1960.
10. Aston, J. G., Misra, B. N., and Cresswell, K. M., *Nature (London)* **208,** 181 (1965).
11. Aston, J. G., and Misra, B. N., *J. Phys. Chem.* **69,** 3219 (1965).

12. ERNST, I. T., GARNETT, J. L., AND SOLLICH-BAUMGARTNER, W. A., *J. Catal.* **3,** 568 (1964).
13. ERNST, I. T., GARNETT, J. L., AND SOLLICH-BAUMGARTNER, W. A., *Aust. J. Chem.* **18,** 993 (1965).
14. ROONEY, J. J., AND PINK, R. C., *Proc. Chem. Soc., London* **1961,** 142.
15. DOLLIMORE, D., AND TONGE, K. H., *J. Chem. Soc. B,* **1967,** 1380.
16. DUNITZ, J. D., AND ORGEL, L. E., *J. Phys. Chem. Solids* **3,** 20 (1957).
17. PAULING, L., "The Nature of the Chemical Bond." Cornell Univ. Press, Ithaca, N. Y., 1960.
18. CORNAZ, P. F., VAN HOOFF, J. H. C., PLUIJM, F. J., AND SCHUIT, G. C. A., *Discuss. Faraday Soc.* **41,** 290 (1966).
19. SLATER, J. C., "Introduction to Chemical Physics." p. 383. McGraw-Hill, New York, 1939.
20. HIRSCHLER, A. E., *J. Catal.* **5,** 196 (1966).
21. MISRA, D. M., *J. Phys. Chem.* **71,** 1552 (1966).
22. GOLUBEV, V. B., AND EVDOKIMOV, V. B., *Russ. J. Phys. Chem.* **39,** 264 (1965).
23. MATSUNAGA, I., AND MCDOWELL, C. A., *Canad. J. Chem.* **38,** 724 (1960).
24. GOLUBEV, V. B., EVDOKIMOV, V. B., AND KIREENKO, G. M., *Russ. J. Phys. Chem.* **39,** 195 (1965).
25. WILLIAMS, D. E., *J. Amer. Chem. Soc.* **88,** 5665 (1966).
26. LORD, N. W., AND BLINDER, S. M., *J. Chem. Phys.* **34,** 1693 (1961).
27. DE BOER, J. H., "The Dynamical Character of Adsorption." Oxford Univ. Press, London/New York, 1968.